

Experiment and simulation analysis of roll-bonded Q235 steel plate

Guanghai Zhao, Qingxue Huang[✉], Cunlong Zhou, Zhanjie Zhang, Lifeng Ma, Xiaogang Wang

University of Science and Technology, Shanxi Provincial Key Laboratory of Metallurgical
Device Design Theory and Technology, Taiyuan 030024, Shanxi, China

[✉]Corresponding author: hqx060913@163.com

Submitted: 12 October 2015; Accepted: 6 February 2016; Available On-line: 21 June 2016

ABSTRACT: Heavy-gauge Q235 steel plate was roll bonded, and the process was simulated using MARC software. Ultrasonic testing results revealed the presence of cracks and lamination defects in an 80-mm clad steel sheet, especially at the head and tail of the steel plate. There were non-uniform ferrite + pearlite microstructures and unbound areas at a bond interface. Through scanning electron microscopy analysis, long cracks and additional inclusions in the cracks were observed at the interface. A fracture analysis revealed non-uniform inclusions that pervaded the interface. Moreover, MARC simulations demonstrated that there was little equivalent strain at the centre of the slab during the first rolling pass. The equivalent centre increased to 0.5 by the fourth rolling pass. Prior to the final pass, the equivalent strain was not consistent across the thickness direction, preventing bonding interfaces from forming consistent deformation and decreasing the residual stress. The initial rolling reduction rate should not be very small (e.g. 5%) as it is averse to the coordination of rolling deformation. Such rolling processes are averse to the rolling bond.

KEYWORDS: Heavy-gauge steel plate; MARC simulation; Roll bonding

Citation / Cómo citar este artículo: Zhao, G., Huang, Q., Zhou, C., Zhang, Z., Ma, L., Wang, X. (2016) "Experiment and simulation analysis of roll-bonded Q235 steel plate". *Rev. Metal.* 52 (2):e069. doi: <http://dx.doi.org/10.3989/revmetalm.069>

RESUMEN: *Análisis experimental y simulación numérica de unión por laminación de planchas de acero Q235.* Planchas de acero Q235 de espesor grueso se unieron mediante laminación y el proceso fue simulado numéricamente utilizando el programa de cálculo MARC. Los resultados obtenidos en ensayos mediante ultrasonidos revelaron la presencia de grietas y defectos en la laminación en una plancha de acero revestido de 80 mm, especialmente en el comienzo y final de la plancha. La microestructura consistía en ferrita+perlita y desunión en la interfase de unión. Mediante análisis por microscopía electrónica de barrido se observó que la interfase contenía grietas con inclusiones. Un análisis de la fractura reveló la presencia de inclusiones no uniformes en la interfase. Además, los datos de simulación utilizando el programa MARC demostraron que había poca tensión equivalente en el centro de la plancha durante la primera pasada de laminación. El centro equivalente aumentó a 0,5 después de la cuarta pasada. Previa a la última pasada, la tensión equivalente presentó poca consistencia en la sección del espesor en la dirección de laminación, impidiendo la unión de interfases y la reducción de la tensión residual. La reducción inicial de la velocidad de laminación no era muy pequeña (en torno al 5%) dado que es contraria a la coordinación de la deformación por laminación. Tales procesos de laminación son opuestos a la unión por laminación.

PALABRAS CLAVE: Planchas de espesor grueso de acero; Simulación numérica MARC; Unión por laminación

Copyright: © CSIC. This is an open-access article distributed under the terms of the Creative Commons Attribution-Non Commercial (by-nc) Spain 3.0 License.

1. INTRODUCTION

There is significant market demand for a large single thick steel plate for applications such as heavy machinery, water conservation, armour and dams. In traditional rolling, heavy ingots are the primary raw materials for heavy plates. However, heavy ingots are thick, and the time for solidification cooling is very long, which leads to serious segregation in the solidification process. Simultaneously, there are serious casting defects of shrinkage cavity, porosity and inclusions at the centre of the heavy ingots due to solidification feeding and volume shrinkage. Using large rolling forces and large reductions in the hot rolling process, the coarse as-cast microstructure can be crushed and defects in the porosity can be partially welded. However, the steel plate will inevitably inherit the original as-cast ingot organization after the rolling process. Consequently, it is difficult to meet high performance requirements for producing large heavy plates, especially for heavy plates that are required to pass z-direction and ultrasonic testing (Luo *et al.*, 2009; Li *et al.*, 2015). Therefore, to examine and prepare thick slabs of material, the JFE Company, on behalf of multiple domestic and foreign research institutes and mills, has researched and developed a variety of manufacturing technologies. Using steel billets welded and manufactured by casting billet and hot vacuum rolling, the JFE Company has successfully produced heavy plates, which satisfy the internal quality requirements of large steel ingots and small compression ratios (Nishida *et al.*, 2005).

Hot rolling bonding makes use of rolling mills to produce composite plates. According to the strong force of the rolling mill combined with the thermal effect, two surfaces of compound metals are pressed together and plastic deformation occurs over the entire metallic cross-section. Simultaneously, the clean and activated surfaces easily form planar metallurgical combinations under the strong rolling pressures. Further, the fundamental difference between the rolling of a composite metal plate and a single metal plate is that the rolling pass of a composite metal plate must be subjected to a large reduction, particularly in the initial rolling pass. This is the only way to promote the physical contact of the composite surface. Therefore, it is necessary

to explore the technology used for manufacturing heavy-gauge steel plates by hot rolling bonds and to further research the processes effects on the properties of heavy-gauge steel plates (Zang *et al.*, 2009; Shen *et al.*, 2011; Yu *et al.*, 2011; Nishimura and Takeuchi, 2014). In this paper, the rolling bond of a heavy-gauge Q235B steel plate was studied, and its organization and mechanical properties were analysed. In addition, the rolling bond process was analysed by nonlinear finite element MARC–MSC software.

2. MATERIALS AND METHODS

2.1. Experimental materials

The raw material is a Q235 casting slab with the chemical composition shown in Table 1.

2.2. Experimental method

First, the billet was prepared and received a surface treatment. The composite surface needs to be clean and ground smooth, which allows the two types of metal atoms to mutually diffuse and achieve metallurgical bonding. Then, the billet was batched and welded with the clean surfaces face-to-face. After implementing high temperatures and long heating times in the chamber furnace, the heavy slab was hot roll bonded using a strong rolling mill. Finally, slow stacking cooling and detection was used for the hot roll-bonded plate. The process is shown in Fig. 1. The initial rolling temperature was controlled from 1020 °C to 1120 °C, and the actual initial rolling temperature was 1056 °C. Table 2 shows the concreteness distribution of the rolling reduction and rolling speed for the hot rolling process under high temperature and low speed and with high rolling reduction. High pressure water descaling was used in the first and second passes in both the initial and final rolling. To retain the steel

TABLE 1. Chemical composition of the experimental Q235B steel (mass fraction, %)

C	Si	Mn	P	S
0.15	0.2	0.55	0.03	0.02

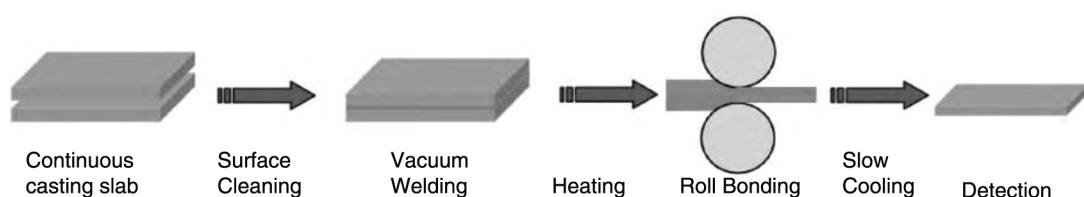


FIGURE 1. Production process for the clad steel plate.

TABLE 2. The hot rolling process

Speed of rolling (r/min)	Thickness before rolling (mm)	Rolling pass (mm)/ Thickness after rolling/ Reduction ratio (%)								Thickness after rolling (mm)
		1	2	3	4	5	6	7	8	
15	400	380	335	280	225	170	120	90	80	80
		5.00	11.84	16.42	19.64	24.44	29.41	25.00	11.11	

TABLE 3. Mechanical properties of the Q235B clad steel plate

State	Yield strength (MPa)	Tensile strength (MPa)	Elongation (%)	Impact energy (J)	Shear strength (MPa)
Control rolling	205	405	24	31	155

straightness, the composite plate needed one or two passes of temper rolling. Composite plates are not control cooled after hot rolling, and the ACC only turned on in the back blowing device. The composite plate was straightened immediately by the straightening machine. Then, it began stack cooling when the temperature dropped to 450–550 °C, and the stack cooling time was greater than 48 hours.

The performance of the composite plate was then analysed. Flaw detection was conducted using an ultrasonic flaw detector according to the GB/T 7734-7734 (Composite plate ultrasonic inspection method). Tensile samples were processed to Standard circular 10×120 mm according to GB/T 228.1-2010 (Metal material tensile test at room temperature); a V-notch standard sample was processed to 10×10×55 mm according to the GB/T 229-2007 (Metal Charpy notched impact test method). A ZBC2602 automatic impact-testing machine was used with a shock temperature of 20 °C. The organization structure and bond interface were analysed using a Carl & Zeiss optical microscope and a scanning electron microscope (SEM), respectively.

3. RESULTS AND DISCUSSION

3.1. Mechanical properties

Using non-destructive ultrasonic flaw detection, cracks and lamination defects were observed in the 80-mm clad sheet steel, especially at the head and tail of the steel plate.

Table 3 illustrates that the hot rolled composite plate did not meet the mechanical properties for Q235 according to GB/T 700-700 (Carbon structural steels). The bonding strength of the composite plate is usually estimated via shear test evaluation, and the shear strength of a layered composite material plate is more than 60% better than a single material plate (Nishida *et al.*, 2005). In this study, the pressure shear test demonstrated that the composite surface shear strength of the rolled plate reached 38.27% of the tensile strength at a given location.

3.2. Analysis of the Microstructure and Bonded Interface

For heavy plate roll bonds, the mechanism of metal interface bonding is primarily mechanical according to film theory and the theory of recrystallization (Boettinger *et al.*, 2000; Ceretti *et al.*, 2009; Cooper and Allwood, 2014). According to these theories, gaps at the interface caused by the machining error are essentially closed during the first rolling pass.

Under high temperature and strong rolling pressure, metal deforms plastically and hardened surface layers are burst. At this moment, the upper and lower fresh metals burst through the cracks of the hardened surface layers and the metal atoms of the fresh metal become mutually embedded in each other. When two groups of metals atoms are within a magnitude of the distance between atoms, atoms are attracted to each other. When adjacent atoms are arranged with stable equilibrium spacing, the free electrons in the outer layers of the two types of metal atoms form metallic bonds. Adding a diffusion layer, formed by diffusible metal atoms at high temperature, achieves a hot rolling bond.

However, the rolling bond is not completed in the first rolling pass. Inclusions still remain in large areas of the interface. There are two reasons for this: first, surface machining and grinding process fail to remove trace oxides, and second, due to the lower free energy at the gap, the resulting precipitates aggregate to form inclusions. With an increase in the rolling reduction rate, there is a rolling compaction effect for the inclusions, causing a discontinuous distribution of the inclusions at the bonding surfaces; however, the shape of the inclusions at the interface is still evident. As the reduction rate continues to increase, the centre of the heavy plate generates plastic strain and the rolling compaction effect on the inclusions at the interface is significantly increased, therefore the previous clear orientation distribution of the inclusions begins to enter a state of dispersion. This greatly weakens the impediments of inclusions for metal bonding. Simultaneously,

more and more grains are formed and the bonding effect gradually improves (Liu, 2010).

Microstructures are shown in Fig. 2. As seen in Fig. 2, there were non-uniform ferrite + pearlite structures in the plate, indicating the lack of consistent plastic deformation in the centre region. Further, there was an unbound area at the interface, indicating that the bonding of the centre portion was inadequate and incomplete under the hot rolling conditions, which corroborates the ultrasonic flaw detection results. Further, the SEM analysis (Fig. 3) reveals long cracks and additional inclusions in the cracks at the bond interface. Serious mixed crystal, cracks and inclusion defects at the bonded interface reduced the mechanical properties of the roll-bonded plate.

3.3. Fracture Analysis

When the inclusion size was large in the interface, the inclusions hindered dislocation slip, leading to dislocation pile, micro-cracks and cracks that occurred during stress concentration, resulting

in brittle fracture at the interface in subsequent stretching processes. However, when the inclusion size was small in the interface, the hindered dislocation slip could be ignored, as it produced ductile fractures (Liu, 2010). Fig. 4a shows that the macroscopic fracture was relatively flush and that necking was not obvious. The microscopic view shows multiple dissociation fractures, and the rest was dimple. There were small inclusions at the dimple bottom, and oxide + MnS identified by EDS analysis showed small inclusions at the bond interface. From the microstructure analysis and the morphology of the inclusions, non-uniform inclusions were found to pervade the bond interface.

4. SIMULATION ANALYSIS

4.1. Finite element models and parameters

In this investigation, simulations of the thick plate production process were analysed using non-linear finite element MARC software. Reversible

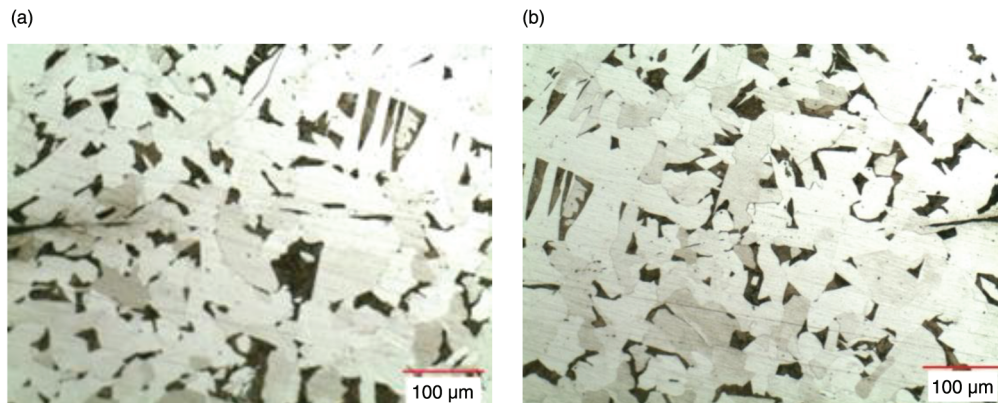


FIGURE 2. Microstructure of the clad steel plate: (a) the head of steel plate and (b) the tail of steel plate.

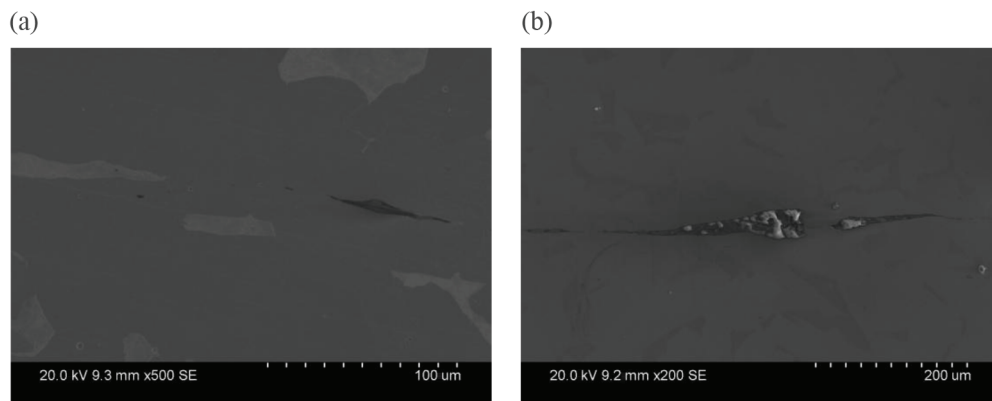


FIGURE 3. Microstructure of the clad steel plate from SEM: (a) with a crack and (b) with a crack and an inclusion.

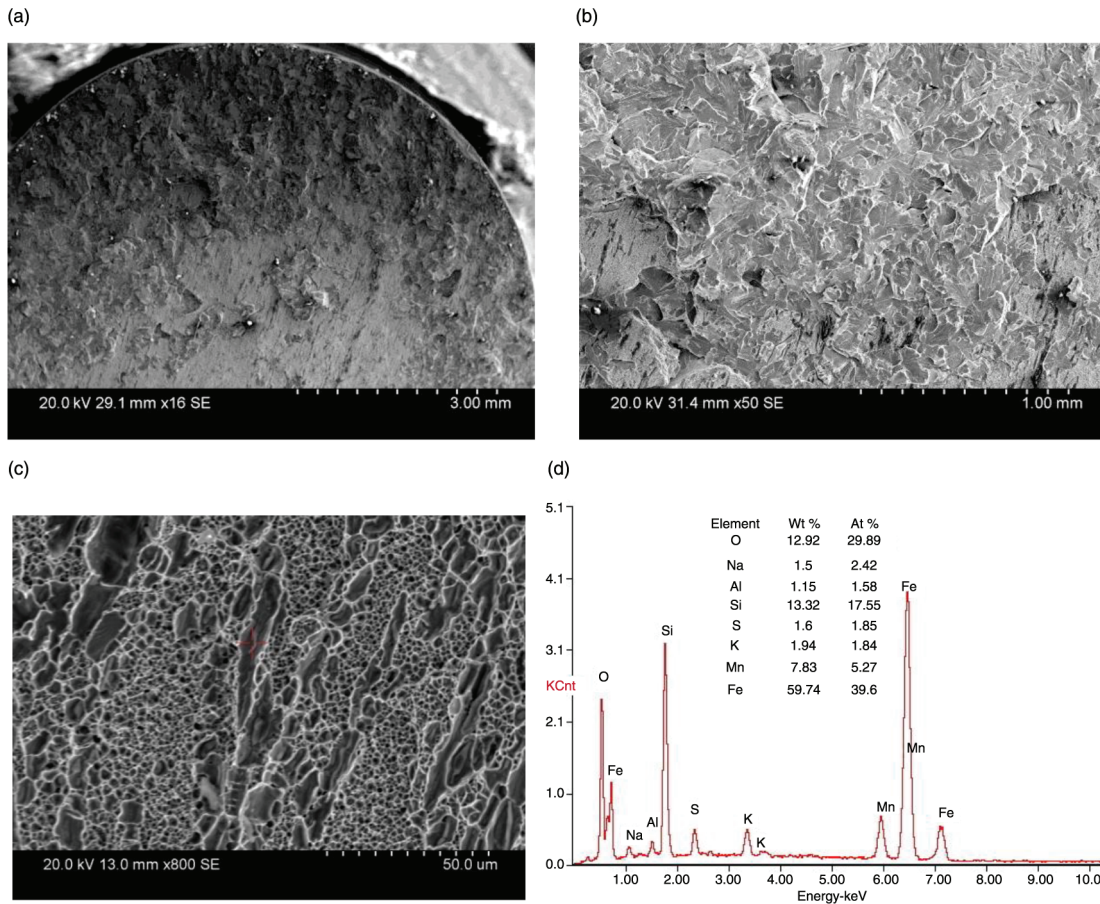


FIGURE 4. Fracture morphologies and EDS analysis of a tensile specimen in the clad steel plate: (a) macro-fractography, (b) cleavage fracture, (c) micro-fracture and (d) EDS analysis of the inclusion for the marked point on the micro-fracture.

hot rolling was simulated using the MARC Model Section simulation (Zhang and Liu, 2015). In this study, the different rolling passes and the equivalent stress and equivalent strain on the thickness direction were analysed. The casting slab of the vacuum hot roll bonding was primarily used to study the deformation across the thickness direction. Its deformation law is the same for the entire slab. Therefore, the entire casting slab was simulated using MARC, according to the actual rolling process simulation (Liu, 2010). Using a 2D model to simulate the actual rolling process, the diameter of the rigid roller was 1000 mm, the slab size was 400×1800×3000 mm; the rolling parameters are shown in Table 2 and the symmetry model is shown in Fig. 5.

4.2. Equivalent stress analysis

When the ratio of the equivalent stress in the rolling process to the yield stress in the current temperature is greater than 1, the metal experiences plastic deformation. As can be seen from Fig. 6, in

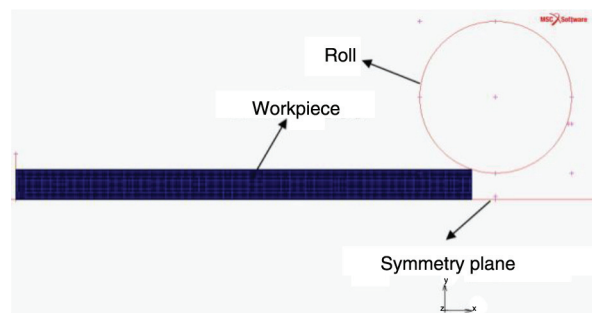


FIGURE 5. FEM simulation model for the rolling process.

the first pass (5% reduction rate), the area with ratio more than one in the centre position was small and the ratio in the rolling gap was uneven. After the fourth pass, the ratio tended to be uniform in the roll gap deformation zone and the large ratio (ratios greater than 2) area began to grow, indicating that the deformation was tending to become increasingly uniform. Prior to the final pass, the ratio was not

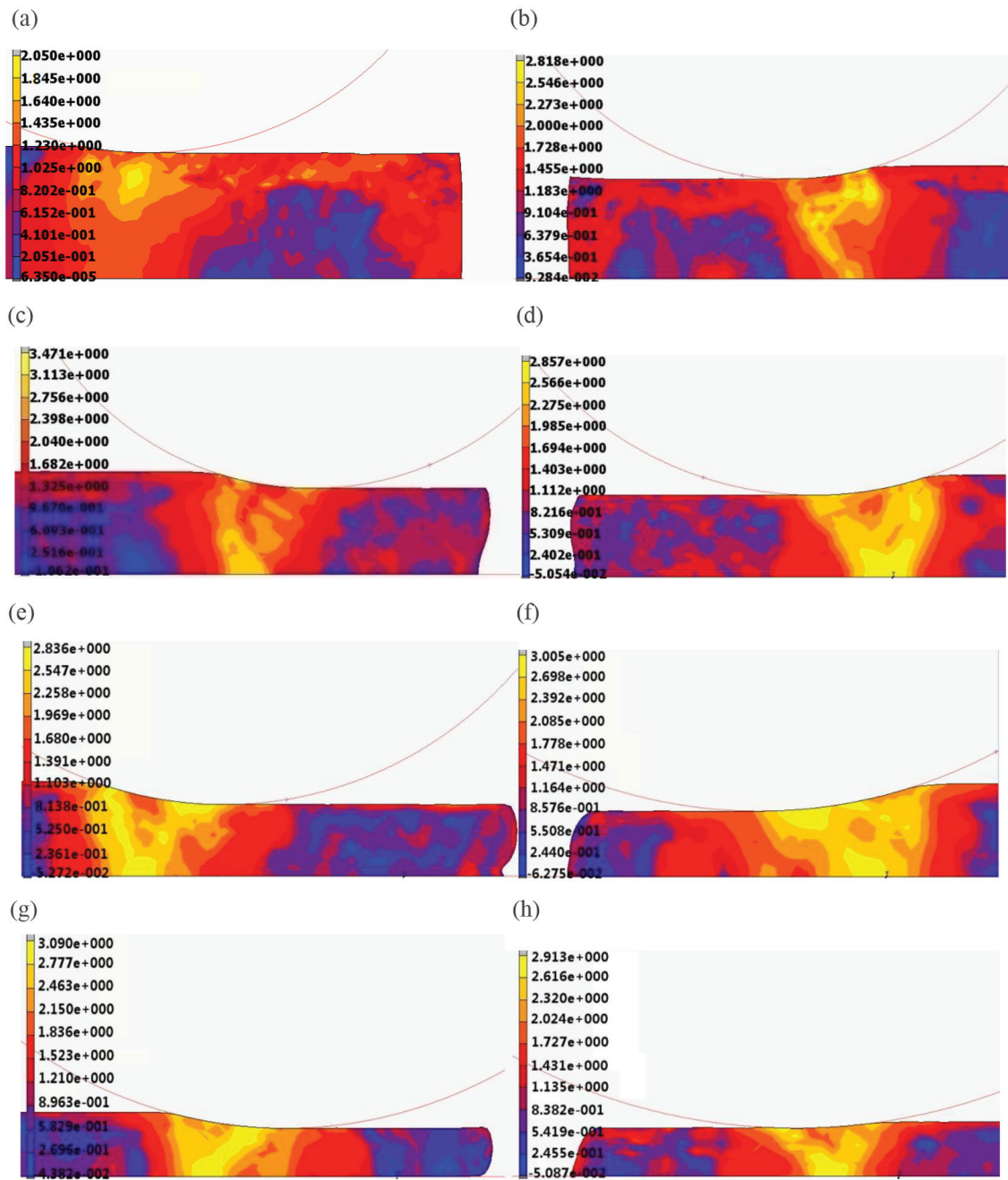


FIGURE 6. Nephogram of the ratio of the equivalent stress in the rolling process to the yield stress in current temperature: (a) first pass, (b) second pass, (c) third pass, (d) fourth pass, (e) fifth pass, (f) sixth pass, (g) seventh pass and (h) eighth pass.

consistent across the thickness direction, which was averse to the bonding interface forming consistent deformation and decreasing the residual stress.

4.3. Equivalent strain analysis

Under high temperature and strong rolling pressures, the metal experienced plastic deformation and the hardened surface layers burst. At this moment, the

upper and lower fresh metal burst through the cracks of the hardened surface layers and metal atoms in the fresh metals became mutually embedded in each other. When two groups of metal atoms are within a magnitude of the distance between atoms, the atoms attract each other. During this process, adjacent atoms were arranged in stable equilibrium spacing, and the free electrons in the outer layer of the two types of metal atoms formed metallic bonds. Adding a diffusion layer

formed by diffusible metal atoms at high temperature, hot rolling bonding was achieved. The exposed active surface was one of the necessary conditions for the bond. Another important factor in the bond was sufficiently high pressure, enough to produce strong shear deformation, forming additional dislocation motion. Therefore, the amount of deformation must be large for each pass of the rolling bond, so as to promote physical bonding components (Takashi and Yasunobu, 2003; Kim *et al.*, 2004).

Using the finite element software MARC, the equivalent strain of each pass was analysed. As seen in Fig. 7, the equivalent strain of the core section was minimal and the equivalent strain close to the surface was maximal on every pass. On the first pass, the plastic deformation of the slab core was small. By the fifth rolling pass, the equivalent strain of the core section increased to 0.5, which is the theorized bond value (Liu, 2010). As the rolling continuing to the eighth pass, the equivalent strain did not tend to

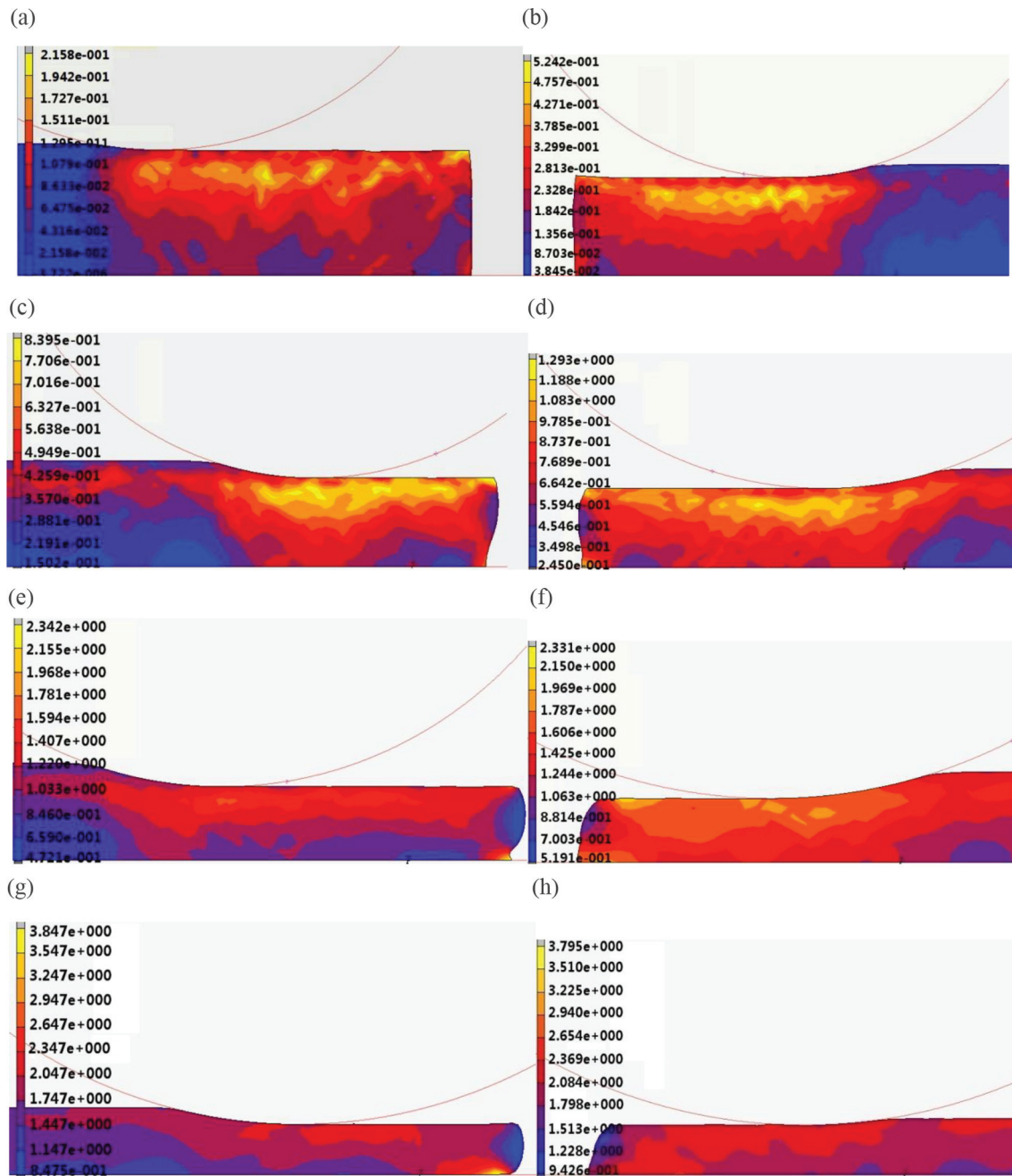


FIGURE 7. Nephogram of the total equivalent plastic strain in the hot rolling: (a) first pass, (b) second pass, (c) third pass, (d) fourth pass, (e) fifth pass, (f) sixth pass, (g) seventh pass and (h) eighth pass.

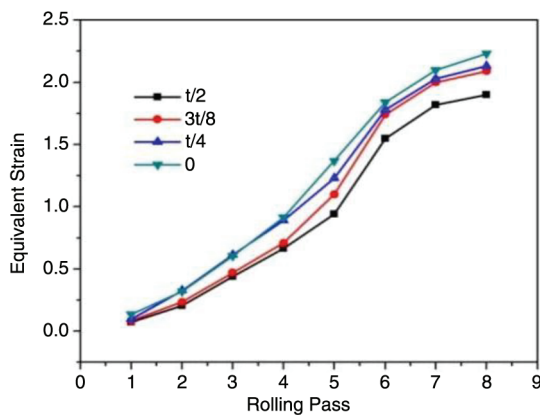


FIGURE 8. Distribution of the equivalent strain in different deformation passes.

be consistent across the thickness direction, which was averse to making rolling deformation in the thickness direction consistent. This law is consistent with the ratio of equivalent stress in the rolling process to the yield stress at current temperature.

Figure 8 shows the equivalent strain diagram from the surface to the heart of the rolled plate (0, $t/4$, $3t/8$, $t/2$). With increasing rolling reduction rate, the difference in the equivalent strain increased from the surface to the heart of the rolled plate. For the first pass (5%), the second pass (11.84%) and the third pass (16.42%), the difference in the equivalent plastic strain was within 0.145 from the surface to the middle of the rolled plate. In the fifth pass (24.44%), the difference was the largest, at 0.428. Prior to the final pass, the difference in the equivalent plastic strain was 0.33. At the initiation of the hot rolling bond, adopting appropriate small rolling reduction rates (12% – 15%) thinned the rolling; then, a large rolling reduction rate of more than 20% was used for the rolling bond in the last several passes to make rolling deformation consistent across the thickness direction, increasing the dispersion of inclusions at the interface and reducing the adverse effects of the inclusion concentration on the plate properties (Liu, 2010). From the above analysis, the initial small rolling reduction rate should not be too small (e.g. 5%), as it would be averse to the coordination of rolling deformation. Such rolling processes are averse to the rolling bond.

5. CONCLUSIONS

Heavy-gauge Q235 steel plate was roll bonded and the process was simulated using MARC software. The ultrasonic testing results revealed that there were cracks and lamination defects in the 80-mm clad steel sheet, especially at the head and tail of the steel plate. There were non-uniform ferrite + pearlite microstructures and unbound areas at the interface. Further, SEM analysis revealed

long cracks and additional inclusions in cracks at the bond interface. Fracture analysis revealed non-uniform inclusions pervading the bond interface. Moreover, MARC simulations showed that in the initial rolling pass there is little equivalent strain in the centre of the slab. With additional hot rolling, the equivalent strain in the centre began to increase to 0.5 by the fourth rolling pass. Prior to the final pass, the equivalent strain was not consistent across the thickness direction, which was averse to the bonding interface forming consistent deformation and decreasing residual stress. The initial small rolling reduction rate should not be too small (e.g. 5%), as it is averse to the coordination of rolling deformation. Such rolling processes are averse to the rolling bond.

ACKNOWLEDGEMENTS

This work was supported by Project U1510131 of the National Natural Science Foundation of China, and the National Key Technology Research and Development Program in 12th Five-year Plan of China (2012CB722801).

REFERENCES

- Boettinger, W.J., Coriell, S.R., Greer, A.L., Karma, A., Kurz, W., Rappaz, M., Trivedi, R. (2000). Solidification microstructures: recent developments, future directions. *Acta Mater.* 48 (1), 43–58. [http://dx.doi.org/10.1016/S1359-6454\(99\)00287-6](http://dx.doi.org/10.1016/S1359-6454(99)00287-6).
- Ceretti, E., Fratini, L., Gagliardi, F., Giardini, C. (2009). A new approach to study material bonding in extrusion porthole dies. *CIRP Ann-Manuf. Techn.* 58 (1), 259–262. <http://dx.doi.org/10.1016/j.cirp.2009.03.010>.
- Cooper, D.R., Allwood, J.M. (2014). The influence of deformation conditions in solid-state aluminum welding processes on the resulting weld strength. *J. Mater. Process. Tech.* 214 (11), 2576–2592. <http://dx.doi.org/10.1016/j.jmatprotec.2014.04.018>.
- Kim, J.K., Huh, M.Y., Lee, J.C., Jee, K.K., Engler, O. (2004). Evolution of strain states and textures during roll-cladding in STS/A1/STS sheets. *J. Mater. Sci.* 39 (16), 5371–5374. <http://dx.doi.org/10.1023/B:JMSSC.0000039247.10346.5d>.
- Li, W.B., Yuan, S.Y., Li, G.L., Wang, C.S., Feng, J. (2015). Microstructure and mechanical properties of low alloy clad heavy steel plate. *Heat Treat. Met.* 40 (6), 49–53. <http://dx.doi.org/10.13251/j.issn.0254-6051.2015.06.012>.
- Liu, J.Y. (2010). Research on deformation rules of heavy gauge steel plate clad rolling. *Northeastern University* 27, 50–54.
- Luo, Z.A., Xie, G.M., Hu, Z.H., Jia, T., Wang, G.D., Wang, L.J. (2009). Experiment study of rolling technology on heavy gauge compound plates. *Journal of Plasticity Engineering* 16 (4), 125–128. <http://dx.doi.org/10.3969/j.issn.1007-2012.2009.04.024>.
- Nishida, S., Matsuoka, T., Wada, T. (2005). Technology and Products of JFE Steel's Three Plate Mills. *JFE Technical Report* 5, 1–9. <http://www.jfe-steel.co.jp/en/research/report/005/pdf/005-02.pdf>.
- Nishimura, K., Takeuchi, Y. (2014). Mechanical Properties Distribution through the Thickness of Heavy Gauge Steel Plate Rolled in Intercritical Region. *Tetsu to Hagane* 100 (9), 1097–1103. <http://dx.doi.org/10.2355/tetsutohagane.100.1097>.
- Shen, J., Li, H., Wang, Y. (2011). Discussion on rolling and processing of extra heavy steel plate with large single piece weight in China. *Wide and Heavy Plate* 17 (2), 23–26.

- Takashi, F., Yasunobu, J. (2003). Rolling technology of composite steel. *Plastic and Processing*, 44 (512), 14–19.
- Yu, W., Zhang, Y.M., He, C.Y., Xu, L.S., Cai, Q.W. (2011). Production of heavy-gauge steel plates by clad rolling process. *J. Univ. Sci. Technol. Beijing* 33 (11), 1391–1395. <http://dx.doi.org/10.13374/j.issn1001-053x.2011.11.012>.
- Zang, Y., Cao, J.N., Hu, X.Z. (2009). The analyzed for the processing way to product heavy plate by ingot. *CSM Annual Meeting Proceedings*, pp. 268–273.
- Zhang, S.H., Liu, J.S. (2015). *Advanced technology and materials processing MSC. Marc realization*, National Defence Industry Press, China, pp. 31–38.